ABSTRACT

Title of Thesis:	BIOMIMETIC POLYMER BASED COMPOSITES WITH 1-D TITANIA FILLERS FOR DENTAL APPLICATIONS
	Rashmi Reddy Mallu, Master of Science, 2018
Thesis Directed By:	Associate Professor, Dr. Isabel K Lloyd, Materials Science and Engineering Department.

The aim of this study was to develop acrylic matrix composites reinforced with one-dimensional (1-D) titanium dioxide (TiO_2) micro and nano fillers that mimic the structure of enamel. To accomplish this, 1-D TiO_2 was synthesized without surfactants or templates using a sol-gel assisted hydrothermal process. Two different approaches were investigated. One used titanium metal powder and yielded TiO_2 rutile microrods. The other used titanium tetraisopropoxide (TTIP) and created TiO_2 anatase nanorods. TiO_2 morphology (size, aspect ratio and state of agglomeration) was affected by glycolic acid concentration and phosphate ion concentration for the titanium metal-based powders, and NaOH concentration for TTIP based powders. Composites were made with silanized TiO_2 micro- and nano-rods in a 50:50 BisGMA:TEGDMA matrix. Organized composites made by injection molding or centrifuging and settling had more uniform mechanical properties (hardness, strength, Young's modulus and toughness) than unorganized composites. Curing the composites under pressure reduced porosity enhancing mechanical behavior.

BIOMIMETIC POLYMER BASED COMPOSITES WITH 1-D TITANIA FILLERS FOR DENTAL APPLICATIONS

by

Rashmi Reddy Mallu

Thesis submitted to the Faculty of the Graduate School of the
University of Maryland, College Park, in partial fulfillment
of the requirements for the degree of
Master of Science
2018

Advisory Committee:
Prof. Isabel K Lloyd, Chair
Prof. Zhihong Nie
Prof. Sreeramamurthy Ankem

Acknowledgements

Firstly, I would like to acknowledge my supervisor, Prof. Isabel K Lloyd, not only for giving me an opportunity to work with her, but for her invaluable guidance, encouragement and support throughout my Masters journey. I am deeply grateful to my advisory committee, Prof. Zhihong Nie and Prof. Sreeramamurthy Ankem for their support, help and constructive advice during my research.

I extend my appreciation to the lab coordinators for their assistance and allowing me to use their facilities. Many thanks to Dr. Peter Y. Zavalij for helping with XRD, Dr. Sz-Chian Liou for his assistance with SEM, Dr. Robert Joseph Bonenberger for allowing me to use polishing and 3-point bend test equipment in their lab. Special thanks go to my colleagues in the lab Dr. Yang Yang, Karan Mohan, Richmond and Daniel for their friendship and help.

I would like to express my heartfelt gratitude to my parents, Ravinder Reddy Mallu and Nancherla Veena for their unconditional love, care and sacrifices throughout my learning journey. I would not have achieved anything in my education and my career without their support. My sincere appreciation also goes to my loving husband, Karthik Reddy Dandu, without his endless support and encouragement; I would not have been able to proceed in my graduate program. Having you by my side gave me the strength and inspiration needed to succeed.

Finally, I could not have succeeded without the support of a Graduate Assistantship from National Institute of Health (NIH) and graduate Teaching Assistantship from Materials Science and Engineering Department, University of Maryland, College Park.

Table of Contents

List of Tables

List of Figures

Chapter 1

Introduction

The introduction of methacrylate resin based micro and nano filler composites revolutionized the field of dental restorative materials and have provided a better alternative to amalgam-based restorations. However, the mechanical and physical properties and resultant clinical longevity of resin based composites (RBCs) have been limited as a consequence of polymerization shrinkage stresses, technique sensitivity and the overall degree of curing of the RBCs. Development and refinement of RBCs through the modification of the filler size and morphology to improve filler loading and distribution has sought to overcome these drawbacks. This has resulted in the introduction of new materials and proposed new material classifications, although the subtle and often incremental modification of filler or resin has often rendered classification difficult.

Innovations in the field of dental restorations over the past few years and the developments in the mechanical and aesthetic properties are discussed in Section 1.1. The structure of natural human enamel and mimicking the structure of the enamel using RBCs including the factors affecting the integrity of the teeth is discussed in Section 1.2. The two main components of the RBCs i.e., polymer material and the filler type are discussed in detail in Section 1.3. The morphology and the fabrication approach affects the properties of the composites including physical, mechanical and aesthetic properties of the RBCs are explained in section 1.4. Surface of the filler material is modified using silane compounds, which is explained in section 1.5. The contribution of titanium oxide fillers in improving the properties of the RBCs and the

reason for choosing the type of the filler is explained in section 1.6. The overall objective of the thesis and hypothesis is described in section 1.7.

1.1 Historical background

Esthetic restorations with natural tooth color and longer lifetime are of utmost importance in the field of dentistry. Research has been going on over the years to find the best match to the mechanical and aesthetic properties of natural human enamel. Silicate cement was the first of the materials used for tooth fillings, by Thomas et al in 1873 [1]. The acidic nature of these silicate cements resulted in pulpal injury and dentine sensitivity [2]. Use of resin-based restorations was introduced in 1940's, but this was associated with high polymer shrinkage due to conversion of monomers to rigid polymers. Incorporation of inorganic fillers to avoid polymer shrinkage was started in 1951 by Knock et al [3]. Bowen first developed a composite containing functionalized silica particles that bonded with bis-GMA in 1963 [4]. This invention revolutionized the industry of dental restorations, which is widely used since. The ensuing development and refinement of resin-based composite (RBC) materials for aesthetic restorative dentistry in the late-twentieth and early twenty-first centuries has led to a wide diversity of materials. These have included Universal RBCs intended for both anterior and posterior placement [5], RBCs containing 'nano-sized' filler particles and described as so-called 'nanofills' [6], highly viscous 'packable' RBCs and also 'flowable' RBCs [7].

1.2 Human teeth:

Human teeth have three layers. From the outside in they are enamel, dentin and the pulp, the living part of the tooth. Both enamel and dentin are hierarchically organized as shown in Figure 1. Enamel, the outer layer, is composed of 90-92% crystalline hydroxyapatite (HA) needles, 1-2% protein, 2-4% collagenous matrix and 4-6% water, while dentin has 25% water including water in tubules, 25% collagenous matrix reinforced with proteins and 50% HA needles [8,9,10]. In enamel, individual HA crystallites (about 20-40nm by 40-60nm by 1600nm) coated with an organic peptide and protein layer self-organize into interlocking prism-shaped HA rods (diameter 4-8μm) oriented with their heads towards the enamel surface. This makes the tooth surface hard, stiff, wear resistant and brittle. The curvy spiraling path of HA rods in the inter rod zone between HA prisms as shown in Figure 2 provides toughness.

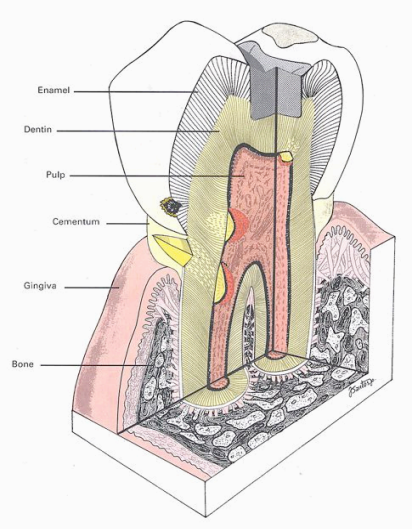

Figure 1: Structure of tooth enamel with filler from Hanning et al, Nature Nanotechnology, 2010, 5, 565 [11]

Figure 2: Micro structure of natural enamel from Nanci, Antoni, ten Cate's Oral history [12]

When bacteria attack the tooth, lesions are formed in the enamel and dentin that must be removed and filled to retain the integrity of the tooth. Ceramic filled polymer matrix composites have largely replaced Ag-Hg amalgam as the material of choice to fill these cavities due to aesthetics and concern about the Hg in amalgam. Posterior fillings (e.g. fillings in molars) are subject to much higher stresses than filling in the front of the month. This study focuses on developing composites that will meet the mechanical and aesthetic requirements of poster restorations.

1.3 Composition of dental composites:

The polymer based composites described in this thesis and the literature consist of two major components, (i) polymer matrix and (ii) filler.

1.3.1 Polymer Matrix:

The polymer matrix for dental composites is typically based on crosslinking dimethacrylates like 2,2-bis[4-(2-hydroxy-3-methacryloyloxypropyl) phenyl] propane (Bis-GMA) ethoxylated BisGMA(EBPDMA); 1,6-bis-[2-methacryloyloxyethoxycarbonylamino]-2,4,4-trimethylhexane (UDMA); dodecanediol dimethacrylate (D_3MA) or triethyleneglycol dimethacrylate (TEGDMA) [13]. When the composite is cured a three-dimensional network is formed by free radical polymerization of the matrix monomers. Polymer shrinkage depends on the monomer used. Polymer shrinkage is higher for low molecular weight monomers, but high molecular weight polymers are highly viscous. Thus, mixtures of different monomers are often used. While the polymer matrix plays a major role, the physical properties of a composite are strongly influenced by the filler material. The

monomer Bis-GMA has been widely used in dental applications since 1960's. Bis-GMA is a very viscous liquid, to improve the handling properties low viscosity TEGDMA can be added. The monomer blend of Bis-GMA and TEGDMA has been approved by the food and drug administration (FDA) and is widely used in both commercial dental composites and for the research purposes. In this work, the polymer matrix used is a blend of Bis-GMA and TEGDMA in a ratio of 50:50.

(a)

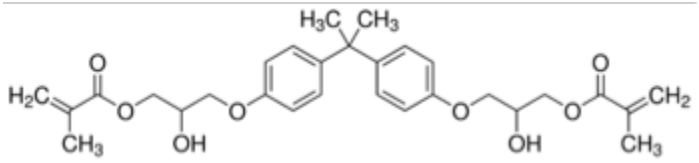

(b)

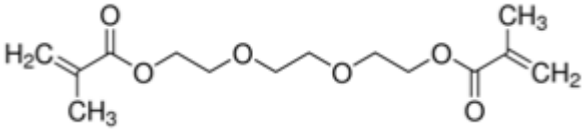

Figure 3: Molecular formula of (a) Bis-GMA (b) TEGDMA

1.3.2 Filler:

Most commonly used filler materials are quartz, colloidal silica, silica glass, strontium and barium glasses or silicates. Inorganic fillers help in improve the strength and the elastic stiffness of the composites. Fillers also help in reducing water absorption, polymerization shrinkage and coefficient of thermal expansion. Bonding of organic and inorganic phases by coating fillers with a coupling agent such as vinyltriethoxysilane and methacryloxypropyltrimethoxysilane (MPTMS) results in the formation of strong covalent bond, which improves the mechanical properties of

the dental composite. The size and shape of the fillers also affects the mechanical and physical properties of the composite. The study conducted by F. Kundie at al. showed that the mechanical properties of the nano filler composites with lower filler loading are superior to that of the micro-filler composites of higher filler loadings [14].

1.4 Classification of Dental composites:

With respect to the filler size, dental composites can be classified into macrofilled, microfilled, hybrid and nanofilled composites [15]. In this thesis, we were working on micro- and nanofiller composites reinforced with TiO_2 nanorods. Microfiller composites consist of bunches of TiO_2 rods with an aspect ratio of 10.5 with uniform rods which replicate the bunch of hydroxyapatite needles in the structure natural tooth enamel. These bunches of microrods were expected to enhance load transfer and increase the Young's modulus of the composite significantly. Nanofiller composites consist of nanorods with lower aspect ratio (5.4). The 1-D nanofillers do not scatter visible light as they shrink to a fraction of this light wavelength (0.4-0.8 μm). So, they are invisible and they can improve the optical properties of composites [16]. Achieving a high volume percentage of nanofillers is challenging as it affects their dispersion in the matrix. Nanocomposite fillers have lower interparticle distances resulting in smooth transition between the stiff inorganic fillers to smooth organic matrix [17, 18]. In contrast, nanofilled composites are characterized by larger interface between the small filler and organic matrix, which results in hydrolytic degradation and a faster degradation of mechanical properties as compared to microfiller composites [19].

1.5 Filler functionalization:

Functionalization of the fillers is done to alter the surface properties and improve the compatibility with the matrix. This helps in forming the link between filler and polymer matrix. Silanization is typically used for functionalizing silicates. It can also be used to functionalize TiO_2. Silanes are silicon chemicals that possess a hydrolytically sensitive center that can react with inorganic substrates to form stable covalent bonds between matrix and the composite and possess an organic substitution that alters the hydrophobicity of the treated surfaces making the particles easier to mix into the uncured matrix. The structure of the silane coupling agent used in this work and its interaction with the filler is given in Figure 4. The process of silanization is more effective with nanofillers than microfillers, as these fillers have higher surface area per unit mass. In a study by Mohsen. N et. Al [47] it was found that the functionalized nanoparticles had a more uniform distribution in the matrix than untreated nanoparticles. The nanoparticles which were not functionalized formed aggregates and nanoclusters. In this work, the silane MPTMS was used as a coupling agent to treat the nano- and micro surfaces.

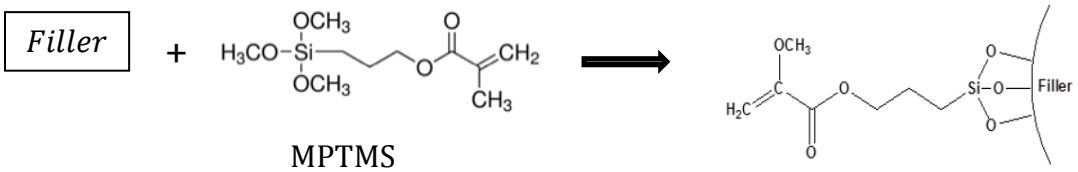

Figure 4: Interaction of the filler and MPTMS

1.6 Titania nanofillers and its biomedical applications

Recent research in synthesizing nanoparticles has focused on controlling the size, shape, crystal structure and surface properties of metal oxides to make them suitable for a wide variety of applications. Increasing interest in synthesizing one dimensional (1D), or rod shaped, metal oxide nanoparticles is due to their potential for applications in electronic [20], optoelectronic [21], electrochemical [22], biomedical [23] and biological [24] devices.

Titanium dioxide (TiO_2) is a versatile ceramic material due to its stability, physical-chemical properties and the ease of production [25]. As a wide bandgap n-type semiconductor material, TiO_2 has been used in dye-sensitized solar cells [26], hydrogen gas sensors [27], photo-catalysts [28], and photodynamic therapy [29]. Because TiO_2 nanoparticles are antibacterial [26], they have also been considered for biomedical applications. TiO_2 particles are white in nature as found in the paints, this property of TiO_2 helps in improving the aesthetic properties of the dental filler. 1D TiO_2 has several advantages over equi-axed or 0D (zero dimensional) particles due to its increased surface to volume ratio, number of delocalized carriers and improved charge transport resulting from the anisotropy of the structures [28]. TiO_2 nanorods are generally synthesized using templates and surfactants that may lead to contamination.

Typically, 1D metal oxides can be obtained by selective rapid growth in a single direction. Some crystals can be easily grown in one dimension due to their strong anisotropic nature. However, TiO_2 crystals require additional energy to produce one-dimensional nanoparticles [32]. Techniques typically used for the

synthesis of TiO_2 include vapor-liquid-solid processes and surfactant controlled approaches involving templates and surfactants respectively [33]. There are two other mechanisms that can be used to grow 1D particles are the oriented attachment mechanism [34] (a solution approach) and the surface reaction limited growth mechanism [35] (a vapor phase approach).

This thesis reports template free and surfactant free synthesis of TiO_2 using sol-gel assisted hydrothermal process for the first time. Our approach for the growth of 1D TiO_2 involves the oriented attachment mechanism. The process is demonstrated using two different precursors, titanium (Ti) metal powder and titanium tetra isopropoxide (TTIP). The effect of the glycolic acid concentration on the aspect ratio and size of the rods is reported. In addition, the effect of ammonium tartrate and ammonium phosphate on the morphology of the rods is discussed.

1.7 Thesis motivation, objectives and hypothesis

To achieve the required mechanical properties, dental composites are highly filled, typically about 60 vol%, with ceramic particles. Current commercial composites have randomly distributed crystalline and glassy silicates with individual particles ranging from 10nm to about 1 μm in diameter [15]. Nanofiller particles are often intentionally agglomerated to enhance mixing, dispersion and solids loading [14]. The filler particles are typically bonded to the resin matrix with silanes to minimize swelling in the oral environment. Clinical performance of these composites can be improved by enhancing mechanical properties, reducing polymer shrinkage (this reduces residual stresses and decreases the gap between the restoration and the

tooth where bacteria could penetrate to cause decay), and increasing biocompatibility. The aim of this research is to improve the lifetime of posterior restorations by increasing the toughness and elastic modulus (to improve load transfer to the tooth) of the composite by mimicking the microstructure of enamel.

The demand for dental composites with longer lifetimes motivated us to work on this project. Nano-TiO2 was identified as a promising reinforcing filler for composites due to its use a white pigment, its elastic modulus, and it potential to inhibit bacterial growth as well as the potential to grow nanorods that could mimic enamel structures. The objective of this study was to introduce n-TiO_2 as reinforcing fillers into a dental composite. This required (i) synthesis of one dimensional TiO_2; (ii) evaluation of the phase and morphology of TiO_2 synthesized; (iii) achieving high filler loading and uniform distribution of fillers; (iv) measurement of the hardness and toughness of the composites with respect to filler type and loading; and (v) evaluation of the effect of autoclave curing on porosity. We hypothesized that using TiO_2 as reinforcing fillers in dental composites would significantly improve their mechanical properties.

Chapter 2

Materials and Methods

2.1 Introduction

In this chapter, the experimental procedures followed in this investigation are described sequentially, and divided into two main sections; (i) synthesis of one dimensional TiO_2 using sol-gel assisted hydrothermal process and its characterization, and (ii) preparation of composites and characterization of their mechanical properties.

The materials used, and the general procedures followed to synthesize TiO_2 micro- and nanorods are described in section 2.2. The nanoparticles were synthesized in a Teflon beaker sealed in a stainless steel autoclave. The autoclave was subjected to heating in heating and drying oven. Detailed information about the experimental set-up used to synthesize the nanoparticles is also reported in this section. Characterization methods for the synthesized materials include: Scanning Electron Microscopy (SEM) and powder X-ray Diffraction (XRD). The detailed information on these characterization methods is described in section 2.3. The reinforced composites were prepared by manual incorporation of silanized titania into the monomer followed by curing as explained in section 2.4 and 2.5. Hardness and toughness of the composite specimens are measured using Vickers' hardness testing and flexural or three-point bending tests.

2.2 Synthesis of Titania micro- and nanorods:

1D TiO_2 particles were obtained by a sol-gel assisted hydrothermal process using metallic Ti powders and TTIP as precursors. At least 5 batches of powder were prepared for each sample type in Table 1 to determine the reproducibility of each technique. The micro- and nanorods synthesized were used for the preparation of polymer-based composites as mentioned in the other sections.

Materials:

Titanium metal powder (< 45 μm), hydrogen peroxide (30 wt% in H_2O), ammonium phosphate monobasic (97%), ammonium tartrate dibasic (<98%), glycolic acid (99%), TTIP (97%), oxalic acid (1 M), acetic acid (3 M) and sodium hydroxide (NaOH). All the chemicals were purchased from Sigma Aldrich and used without further purification.

Methods:

Metallic Ti powder approach: 1.732 grams of Ti powder was dissolved in 50 ml of 30 wt% hydrogen peroxide, which served as an oxidizing agent, using magnetic stirrer for about 6 hrs forming a titanium peroxo complex. Then, 1.5 wt% of glycolic acid was added with 5 wt% of ammonium tartrate or 5 wt% of ammonium phosphate forming a peroxo-titanium-glycolate complex. After this gel was formed, it was dissolved in deionized water to form 100 ml of total solution. Next additional glycolic acid, 1.5 wt% or 3 wt%, was added to evaluate the effects of excess glycolic acid and lower pH on inhibition of TiO_2 growth in some crystallographic directions. The process and the parameters are illustrated in Figure 5 and Table 1.

TTIP approach: 2.53 grams TTIP was added to 42 ml oxalic acid such that there was a 1:4.6 mole ratio of oxalic acid solution (1M) to TTIP. Then the TTIP was dissolved using a magnetic stirrer. After the TTIP was dissolved in the oxalic acid, either 8 grams or 16 grams of NaOH was added to form a gel.. Then the gel was then dissolved using deionized water (DI) to form 125 ml solution of titanium oxalate in deionized water. This process is illustrated in Figure 6.

The solutions obtained in both the approaches were transferred to a 300ml Teflon vessel and sealed in a stainless steel autoclave and autoclaved at 453K for 48 hrs. Then, the precipitates that formed were washed using deionized water and ethanol. Firstly, they were washed using 100 ml of ethanol for two times and then washed using 100 ml of deionized water for three times. After each washing step, the TiO_2 particles were separated using a centrifuge at 26°C and 9500 rpm. They were then dried at 80°C for an hour. Table 1 shows the four titanium oxide different powders made from variations in the metal precursor process and the two different titanium oxide powders made using the TTIP precursor process.

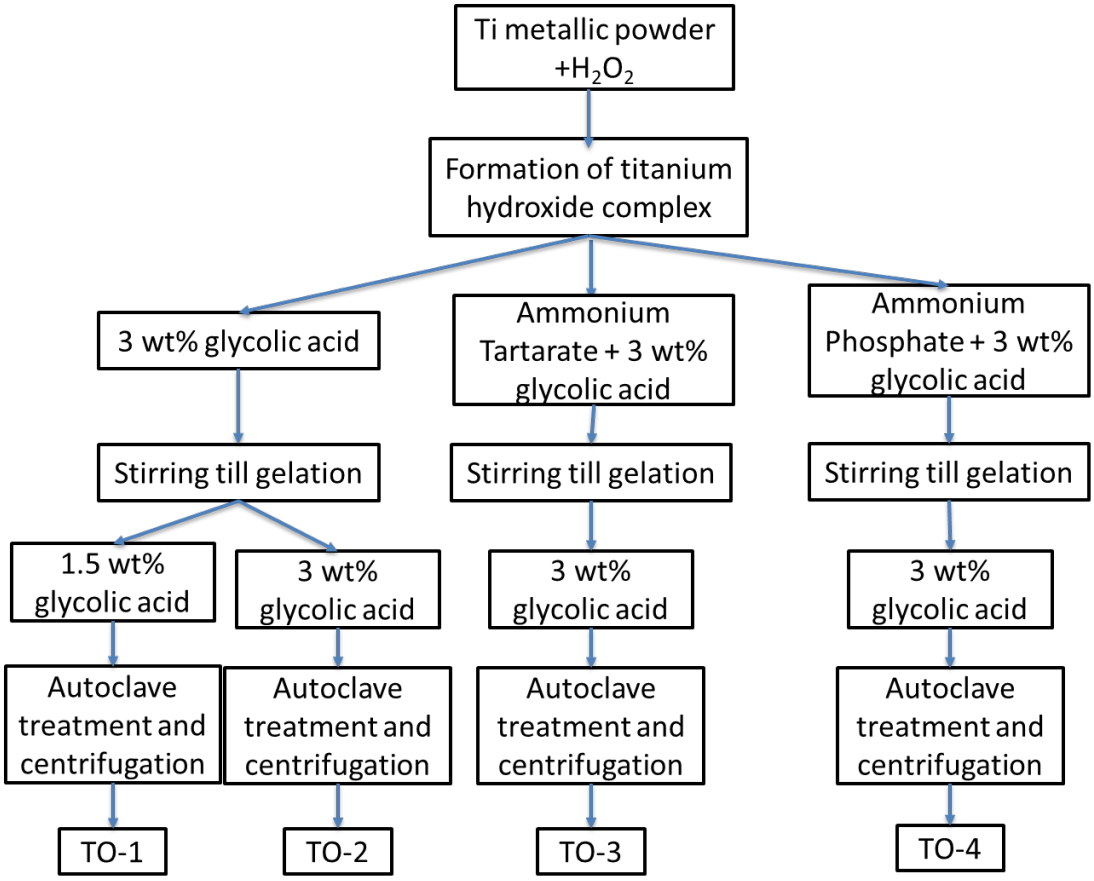

Figure 5: Flowchart for synthesis from metal powders

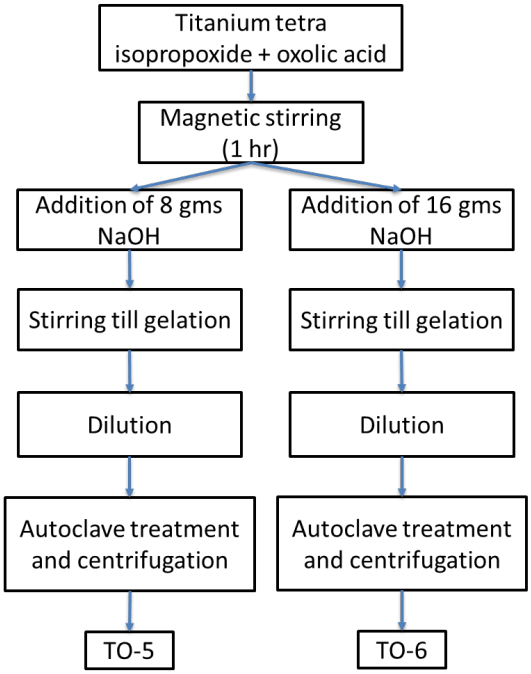

Figure 6: Flowchart for synthesis from TTIP

Table 1: process parameters of the TiO_2 samples synthesized.

Composition	**Precursor used**	**Process parameters**
TO-1	Ti metal	1.5 wt% excess glycolic acid
TO-2	Ti metal,	3 wt% excess glycolic acid
TO-3	Ti metal	3 wt% excess glycolic acid + 1.5 wt% ammonium tartrate
TO-4	Ti metal	1.5 wt% excess glycolic acid + 1.5 wt% ammonium phosphate
TO-5	TTIP	8 gms of solid NaOH pellets
TO-6	TTIP	16 gms of solid NaOH pellets

2.3 Characterization Techniques for TiO_2:

2.3.1 X-ray diffraction (XRD):

XRD was carried out using CuKα radiation (30 kV, 10 mA) to examine the TiO_2 crystalline phase following synthesis. The samples were prepared for XRD by gentle grinding 0.1 g of the powder using a mortar and pestle. The powder was placed evenly on a plastic XRD flat plate and placed in the XRD machine. Data were collected at a scattering angle of 2θ from 10° to 80° with 0.05° step size and 10°/min scan speed (BRUKER AXS D2 phaser, Karlsruhe, Germany). 2θ for equivalent CuKα radiation was calculated using Bragg's Law [36]. The average crystallite size was calculated using the Scherrer formula (2) by obtaining line broadening.

$$D_v = K \lambda / \beta \cos\theta \qquad \text{Eq (1)}$$

Where; D_v is the average particle size, λ is wave length of the radiation and β is the FWHM(full width at half maximum) of the reflection peak that has the same maximum intensity in the diffraction pattern (integral breadth of the peak ocated at angle θ). K is the Scherrer constant. The Scherrer constant (K) in the formula accounts for the shape of the particle and is generally taken to have the value 0.9 [37]. The size obtained from the Scherrer formula yields the apparent or average crystallite size for a material. Powders are often polycrystalline so that the crystallite size may be smaller than the measured particle size.

2.3.2 Scanning electron microscopy (SEM):

SEM was used to evaluate the morphology and estimate the size of the TiO_2 powders (SEM, LEO (Zeiss) 1540XB). Samples were prepared for SEM by dispersing small amount of TiO_2 powder in 190 proof ethanol and coating it on a silicon wafer. These silicon wafers were mounted on SEM stubs using carbon tape.

2.4 Functionalization of TiO_2:

TiO_2 micro- and nanorods were acid washed using glacial acetic acid and then functionalized using silane compounds, in a process commonly known as silanization. During the process, 1-D TiO_2 was dispersed in ethanol with 10% deionized water. The silane compound Methacryloxypropyltrimethoxysilane (MPTMS) was added. The reacting mixture was kept under constant stirring at room temperature for 18 hrs. The reacting mixture was then placed in a heating and drying oven at a temperature of 80°C, to evaporate the solvent and dry the reaction product

The synthesized TiO_2 (TO-4 and TO-5) was dispersed in 200 mL ethanol and 100 mL deionized water. The silane-coupling agent MPTMS was added to the solution mixture on magnetic stirrer. The reacting materials were kept under constant stirring at room temperature for 24 h. The mixture was then subjected to centrifuging at speed of 9000 rpm for 15 minutes to separate out the solvent. Afterwards, the reaction product was subjected to drying at 80°C overnight. Earlier studies suggested that using 10% silane is more than enough to coat the filler surfaces completely. The amount of silane required to coat the filler was calculated using the following equation [17]: $X = (A/\boldsymbol{\omega})\ f$, where X is the amount of silane (g) needed to coat the

fillers, A is the surface area of the filler (m^2/g), **ω** is the surface area coverage per gram of silane (m^2/g), and *f* is the amount of filler (g). In the case of TiO_2 used in this study, the surface area A= 330 m^2/g and the surface area 30 coverage per gram of silane ω = 2525 m^2/g [17]. Therefore, the amount of silane used to coat 1 g of micro TiO_2 (TO-4) in this work was 0.13 g. The amount of silane required to coat nano TiO_2 (TO-5) was higher than TO-4, as the surface area increases with decrease in particle size.

2.5 Mixing and curing of composites:

2.5.1 Materials:

Resin Matrix: 50:50 w/w BisGMA (Esstech): TEGDMA (Sigma-Aldrich); Benzoyl peroxide (BPO) catalyst (Acros Organics)

Synthesized Fillers: Titanium oxide micro- and nanorods (TO-4 and TO-5)

2.5.2 Processing:

Mixing:

TEGDMA was added to BisGMA to create a 50:50 w/w stock monomer mixture. The monomer was activated with 1wt% BPO. All the composites had a 50:50 w/w BisGMA:TEGDMA matrix. To achieve high filler loading, ethanol was added to the resin matrix a drop at a time using pippette as a diluent. The filler was folded into the matrix in small batches. When mixing was complete, the diluent was allowed to evaporate for 24-48 hrs depending on the amount of ethanol used for mixing.

Table 2: Types of composites characterized

Composite	Filler	Percentage of filler (Volume %)	Organization	Curing
1	TO-4	58	Unorganized	Hot air oven
2	TO-4	54	Unorganized	Autoclave curing
3	TO-4	54	Organized (injection molding)	Autoclave curing
4	TO-5	56	Unorganized	Hot air oven
5	TO-5	56	Organized (centrifuging)	Hot air oven
6	TO-5	56	Organized (injection molding)	Hot air oven
7	TO-5	56	Organized (injection molding)	Autoclave curing

Molding:

All the composites prepared had a 50:50 w/w BisGMA:TEGDMA matrix. Unorganized composite three point bend test bars were made by packing composite into 4mm*4mm*25mm nylon molds. Organized composites were prepared by centrifuging and injection molding. Bars were made from centrifuged TO-5 filler and monomer mixture by curing the composite in the centrifuging tube. The cured composite from centrifuging tube were cut into bars of size 4mm*4mm*25mm. The injection molded composites were prepared using both TO-4 and TO-5 in the monomer matrix. The monomer and the filler mixture flows through the plastic tube to the nylon molds of size 4mm*4mm*2mm.

Centrifugation to organize TO-5 titania nanorods:

The monomer blend Bis-GMA and TEGDMA was initially added to the centrifuging tube. TO-5 powder was then added to the blend 0.5 mg each time and mixed and dispersed to form a paste, until it reaches the mixture was too stiff to stir. Then 2ml of ethanol was then added in order to facilitate the movement of the nanorods during centrifugation. Organized composite bars were made with 85 wt% (56 Volume %) of TO-5. The TO-5 filler was folded into the matrix in small batches. The composite mixture was centrifuged at a speed of 10,000 rpm for 30 min. After centrifuging the tube containing the monomer mixture is left undisturbed for 48 hrs to evaporate solvent. The sample is then subjected to curing in the centrifuging tube at 90°C for 4 hrs. The experiment was repeated for four times and four bars were cut from the centrifuging tubes.

Injection molding of TO-4 and TO-5 composites:

The experimental setup for injection molding consists of plastic conical tube with a piston to apply pressure, a plastic pipette and a polymer mold. A plastic pipette was attached as a tube at the mouth of the narrow end of the conical tube. The pipette was directed into the molds. The monomer mixture, filler and the diluent were mixed manually and were allowed to flow through the experimental setup. The microrods were organized during the flow through the nozzle of the conical plastic tube with application of pressure using piston from the other end of the tube and then through the pipette. The schematic for the injection molding set up is shown Figure 7. The molds are then left in the hood undisturbed for 48 hrs to evaporate the solvent.

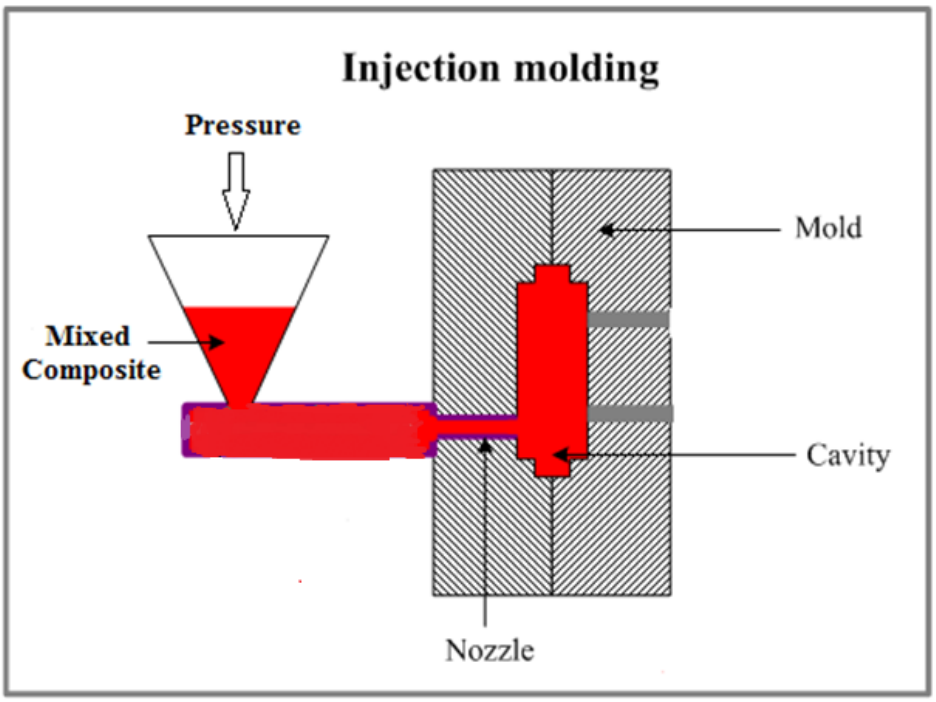

Figure 7: Schematic of injection molding equipment

The molds used to shape the organized composites are of two types. The 4mm*4mm*25mm nylon molds were used to shape the composites for three-point bend tests. These molds require about 4 grams of uncured composite. Smaller molds, which hold about 1 gram of the uncured matrix, were used for preliminary tests to evaluate curing behavior and Vickers hardness. These molds were 1 mm high and 1 mm in diameter.

Curing:

All of the composites were cured before characterization. When ethanol was added as a diluent it was allowed to evaporate before curing as noted above. Most samples were cured under atmospheric pressure at 120°C for 4 hrs. A limited number

of samples in the small molds were cured in an autoclave to evaluate the effects of constant pressure during curing. To evaluate the effects of pressure on curing, a small mold containing monomer and filler mixture is transferred to a 300 ml Teflon vessel. This vessel is then sealed in a stainless steel hydrothermal autoclave and cured at 120°C in the heating and drying oven for 4 hrs.

Polishing:

The composite samples were polished manually. First they were glued on aluminum stubs using Aremco Crystalbond. Then they were ground and polished on one side to make sure they were flat and parallel. The samples were initially ground using silicon carbide disks of size 320, 600 and 1800. Polishing cloth and diamond suspensions of sizes 6 μm, 3 μm and 1 μm were used for the final finish. Then the sample was removed from the stub and turned over so that opposite face could be polished. Then edges were polished. Samples in small molds were only polished on the two parallel surfaces.

2.6 Characterization of composites:

2.6.1 Scanning Electron Microscopy (SEM):

Cross sections of the cured composites were imaged to determine the short and long range ordering of the filler. A Hitachi SU-70 Schottky field emission gun SEM was used for all the studies. The polished samples are mounted on a stub using carbon tape. These samples are carbon coated using Agar SEM carbon coater in order to increase the conductivity of the samples. Short-range order and long-range order were characterized using higher and lower magnifications respectively. Long range

order was observed in a magnification range of 30x-50x magnification whereas short range order was observed in the range of 600x to 35,000x magnification.

2.6.2 Vickers Hardness Test:

A Vickers hardness tester Wilson® VH1102 Micro Hardness Testers was used to measure hardness. It has a load cell and square pyramidal diamond indenter. A load of magnitude 9.8 N was applied to a flat surface and polished surface to determine the hardness. After the load is removed the filar eyepiece is then adjusted to measure the diagonals of the indentation. The Vickers Hardness (HV) number is then determined by the automated system. The formula used for determine the HV number is given by:

$$\mathrm{HV} = \frac{\mathrm{F}}{\mathrm{A}} \approx \frac{1.8544\ \mathrm{F}}{\mathrm{d}^2} \qquad \text{Eq (2)}$$

Where F is the load applied (kg), A is the area of indentation and d is the diagonal of square indentation (mm). Indentations were taken about 0.2 mm apart from each other on the polished surface of the cured composite. At least 5 measurements were taken for each sample, these readings are averaged and standard deviation is calculated.

2.6.3 3-Point Bend Test:

Composite bend bars (roughly 3mm by 3 mm by 25 mm after polishing) were tested in three point bending to determine elastic modulus (E); flexural strength (FS); toughness (UT, area under stress-strain curve).

Polished specimens were subjected to transverse loading to determine the maximum load required for fracture. The measurements were performed using a universal testing machine (Zwick/ Role, Leominster, UK) at cross head speed of 1mm/minute. The specimens were placed on fixtures on universal test machine

between the supports (L). The flexural strength was expressed as maximum flexural load pre-cross-sectional area of specimen (MPa), according to international standards organization (ISO 4049). The values of flexural strength were obtained from three points bending test, in (MPa), based on the following formula:

$$\text{Flexural strength} = \frac{3FL}{2bh^2} \qquad \text{Eq (3)}$$

Where F is the force load at fracture point (N), L is the length of support span (mm), d thickness (mm), and b the width of specimen (mm). The Young's, or elastic, Modulus and the toughness are calculated using the program written by Beth Wyler using MatLab. The strain-strain curves are also plotted using the same program. For the calculation of toughness of the composites, the range of the toughness for each value is calculated and then averaged, which gives the original toughness of the composites.

Chapter 3

Results

This chapter describes the results of the characterization of the 1-D TiO_2 powders that were synthesized and the composites that were made from them. In particular, it gives results for the size and shape and crystallite size and phase of the TiO_2 nano- and micro-rods and the microstructure and mechanical of the composites made from them.

1D TiO_2 powders were characterized using XRD and SEM. The XRD patterns with diffraction peaks identified in terms of phase and plane are shown in Figure 7 and 8 of section 3.1.1. The crystallite sizes for the titania powders calculated using half width full maxima of the diffraction peaks are given in Table 3. SEM images showing the morphology of the TiO_2 synthesized are shown in Figure 9-10. The diameter and length of the particles calculated from the SEM images that are in Table 4.

The composites synthesized were characterized using SEM, Vickers hardness and 3-point bending. SEM images of the organized (injection molded and centrifuged) composites and the difference in porosity of the composites cured at atmospheric pressure and under controlled pressure are shown in Figures 12 and 13. Vickers hardness values given in Table 5 allow comparison of hardness for organized and unorganized composites. Table 6 shows the values of Young's modulus, flexural strength and toughness for centrifuged samples and unorganized samples made using TO-5 nanorods. The stress strain curves corresponding to these values are given in Figure 14.

3.1 Characterization of 1-D TiO_2:

3.1.1 X-Ray Diffraction:

All of the precipitated TiO_2 powders were white. X-ray diffraction was used to determine the phase assemblage and average crystallite size of each of the powders. Figure 7 shows representative XRD patterns between 20-80° 2θ for the Ti metal derived compositions in Table 1. Analysis of the X-ray patterns in Figures 7a and 7b shows that the TO-1 and TO-2 powders consist of both anatase and rutile with trace amounts of brookite. The diffraction patterns in Figures 2c and 2d matched the peaks of the rutile phase of TiO_2. No anatase or brookite peaks were found. Figures 7b, 7c and 7d show that the TO-2, TO-3 and TO-4 powders have narrower peaks than TO-1 in Figure 7a. This indicates that the powders had a larger crystallite size than TO-1.

Figure 8 shows the XRD patterns for the TTIP derived titanium oxide powders in Table 1. TO-5 in Figure 8 has very broad peaks including a prominent peak at 25° which belongs to the anatase phase. The peak broadening for this powder is because of the very small crystallite size of this powder. In Figure 8 b for TO-6, there are peaks for all three phases of TiO_2, rutile, anatase and brookite. Table 3 summarizes the crystallite sizes of the different phases of the TiO_2 formed in under each of the processing conditions.

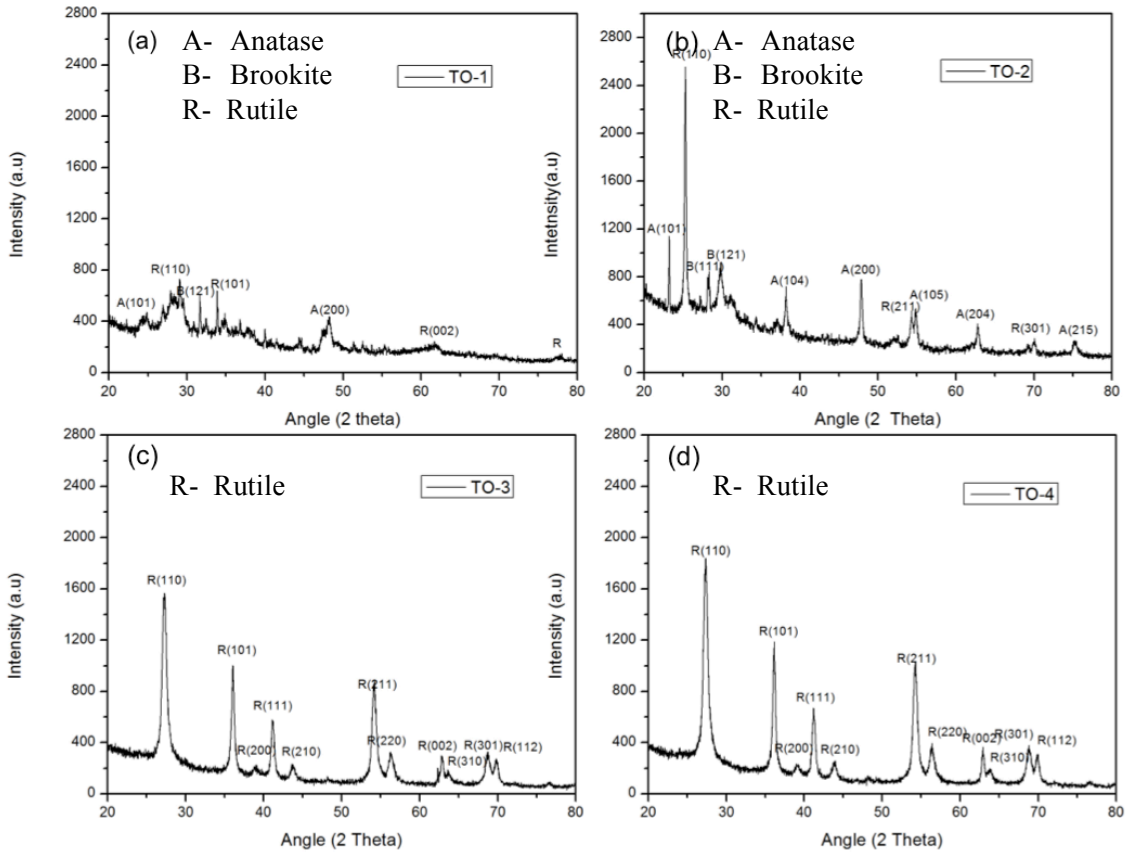

Figure 8: XRD patterns of TiO_2 particles with various crystalline phases (a) TO-1, (b) TO-2, (c) TO-3 and (d) TO-4

(a)

(b)

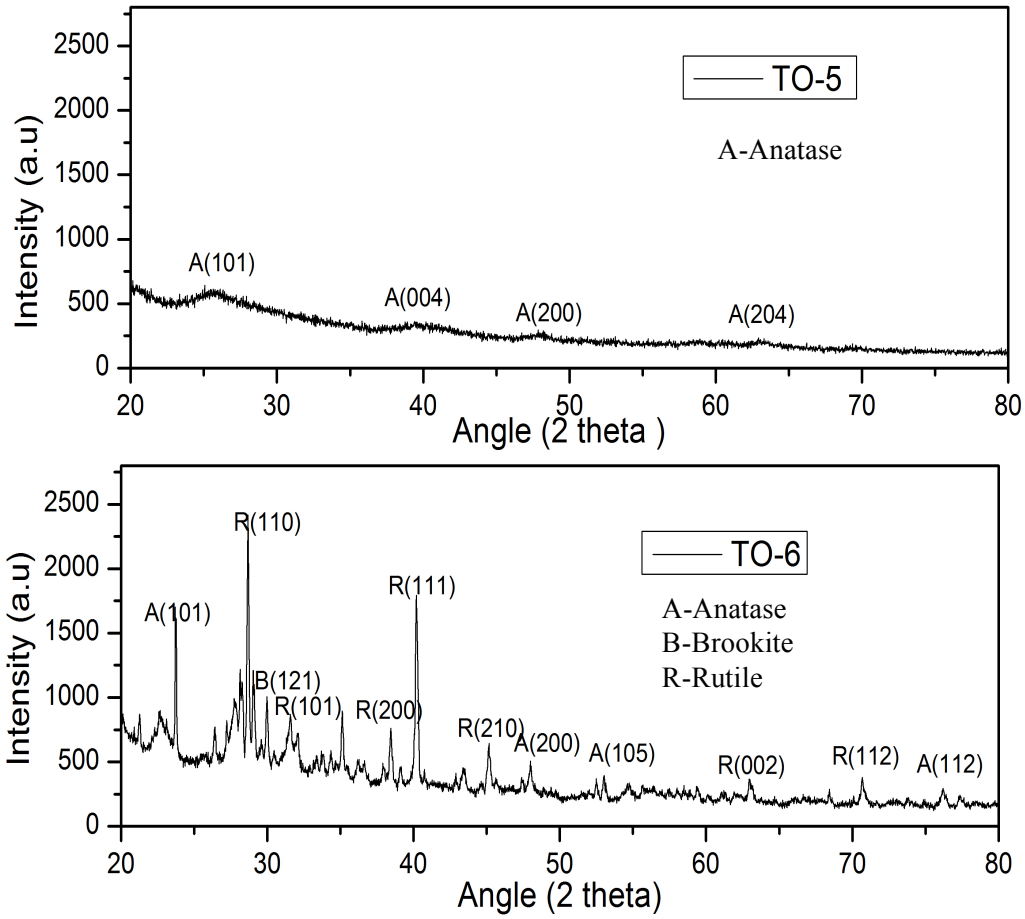

Figure 9: XRD patterns of TiO_2 particles with various crystalline phases (a) TO-5 and (b) TO-6

Table 3: Phases formed and the crystallite size of the anatase and rutile phases.

Composition	Phases present	Crystallite size of Anatase (nm)	Crystallite size of Rutile (nm)
TO-1	Rutile (major phase), Anatase (minor phase)	8.12	7.5
TO-2	Rutile (major phase), Anatase (minor phase)	27.88	23.93
TO-3	Rutile	-	19.37
TO-4	Rutile	-	18.05
TO-5	Anatase	3.11	-
TO-6	Anatase, Rutile	36.93	37.63

3.1.2 Scanning Electron Microscopy (SEM):

Figures 9-11 illustrate the effects of the glycolic acid, ammonium tartrate, ammonium phosphate and NaOH additions on the morphology of the powders derived from Ti metal and TTIP. In Figure 9, the differences in morphology between TO-1 and TO-2 can be clearly observed. TO-1 had heavily agglomerated short rods while TO-2, which had twice as much glycolic acid as TO-1, had much larger longer needles that were less heavily agglomerated. Figures 10a and 10b show that the addition of ammonium tartrate led to high aspect ratio TiO_2 micro-rods with hexagonal cross-sections that tended to be heavily agglomerated in haystack bundles. Figures 10c and 10d show that adding ammonium phosphate resulted in rutile powders that consisted of linear bundles of TiO_2 microrods. Unlike composition TO1-

TO4, compositions TO-5 and TO-6 were synthesized from TTIP with NaOH added to promote the development of anisotropic rods. Figure 11 shows that TO-6 powders made with the higher concentration of added NaOH were larger and had a larger aspect ratio than the TO-5 powders. Both powders were processed for the same length of time. The average length and diameter of the synthesized nano- and micro-rods and their standard deviation were calculated using ImageJ software downloaded from NIH. The values are shown in Table 4. The effect of process parameters on the aspect ratio of the 1D TiO_2 is discussed in detail in section 4.3.

Table 4: Average diameter of the TiO_2 micro- and nanorods

Sample	Average Diameter	Average length
TO-1	42 ± 7 nm	64 ± 13 nm
TO-2	156 ± 4 nm	11 ± 0.2 μm
TO-3	2.1 ± 0.2 μm	41 ± 0.3 μm
TO-4	2.0 ± 0.02 μm	21 ± 0.01 μm
TO-5	8 ± 1.5 nm	42 ± 3.3 nm
TO-6	95 ± 42 nm	1.7 ± 0.6 μm

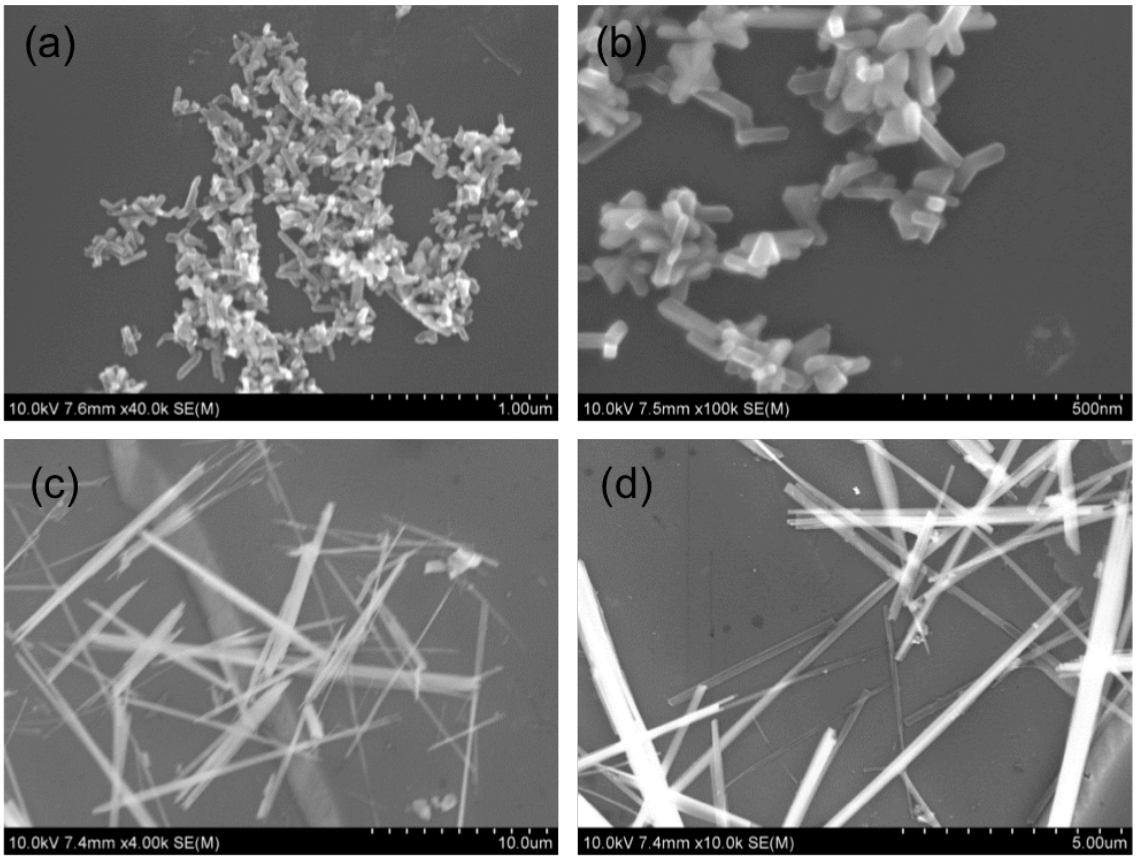

Figure 10: SEM images of TiO_2 nanorods synthesized using Ti metal powder and glycolic acid: (a) and (b) TO-1 (1.5 wt% of glycolic acid), (c) and (d) TO-2 (3.0 wt% of glycolic acid).

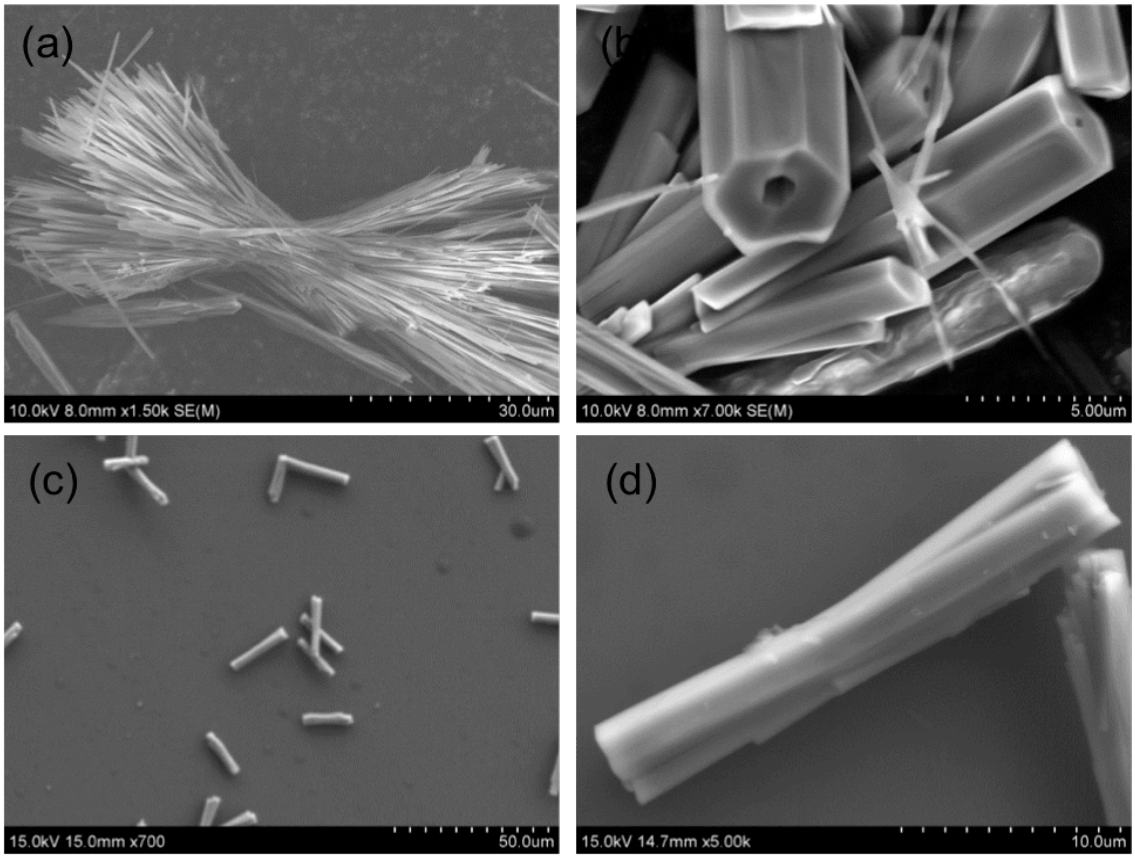

Figure 11: SEM images showing effect of ammonium compounds on the morphology of titanium oxide (a) and (b) TO-3, ammonium tartrate, (c) and (d) TO-4, ammonium phosphate.

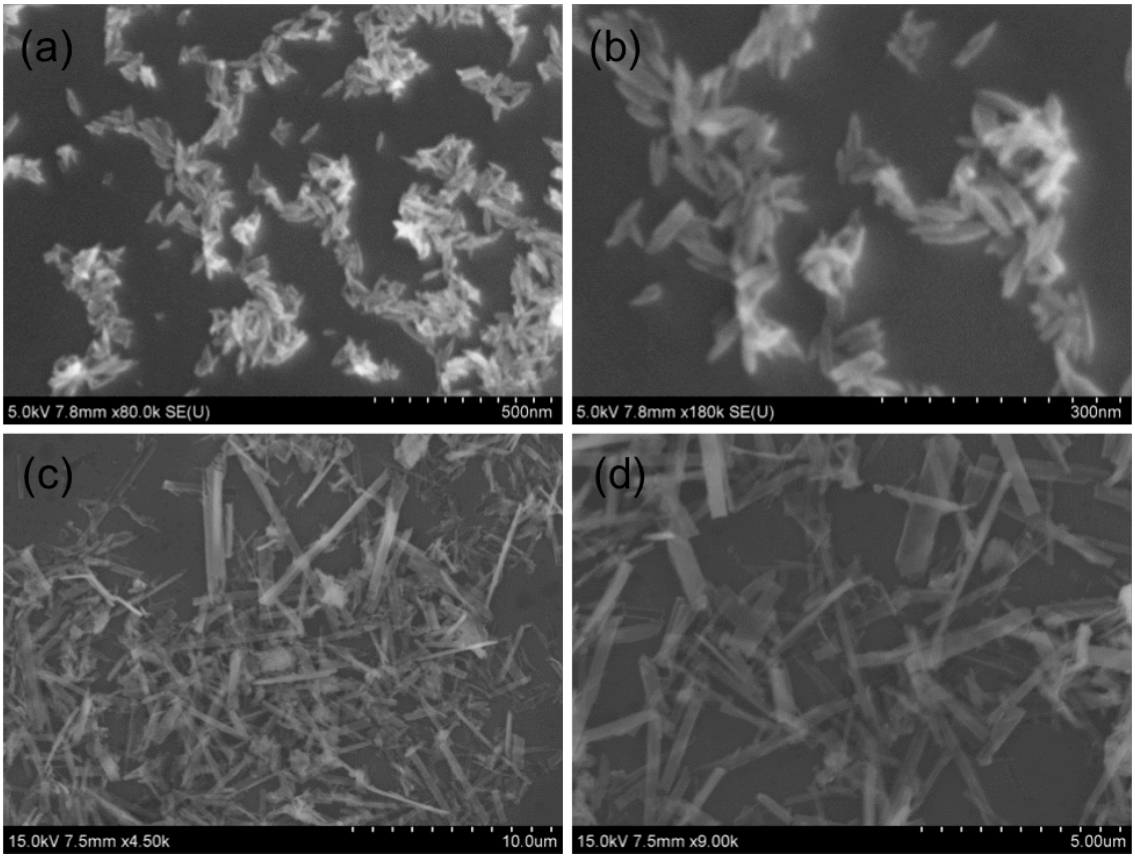

Figure 12: SEM images of TiO_2 nanorods by the addition of NaOH (a) and (b) TO-5, 8 grams NaOH, (c) and (d) TO-6, 16 grams NaOH.

3.2 Morphological characterization of reinforced composites

3.2.1 Scanning electron microscopy:

Injection molding and centrifuging resulted in the uniform distribution of filler in the polymer matrix that can be seen in Figure 12 (a) and (b) respectively. Figure 12(a) shows a composite with bundled TO-4 microrods. These composites were used to explore orientation of the 1D fillers using injection molding. It can be seen that the microrods are arranged in 2-D space rather than 3D because the injection molding tended to orient the micro-rod bundles in the same plane. The micro-bundles are oriented in different directions parallel to the injection molding flow direction but they appear to be uniformly distributed. Figure 12(b) shows a composite prepared with TO-5 nanorods that were organized by centrifuging after the composite was mixed by hand. The nano-rod heads are perpendicular to the surface. It can be seen that centrifuging results in uniform distribution.

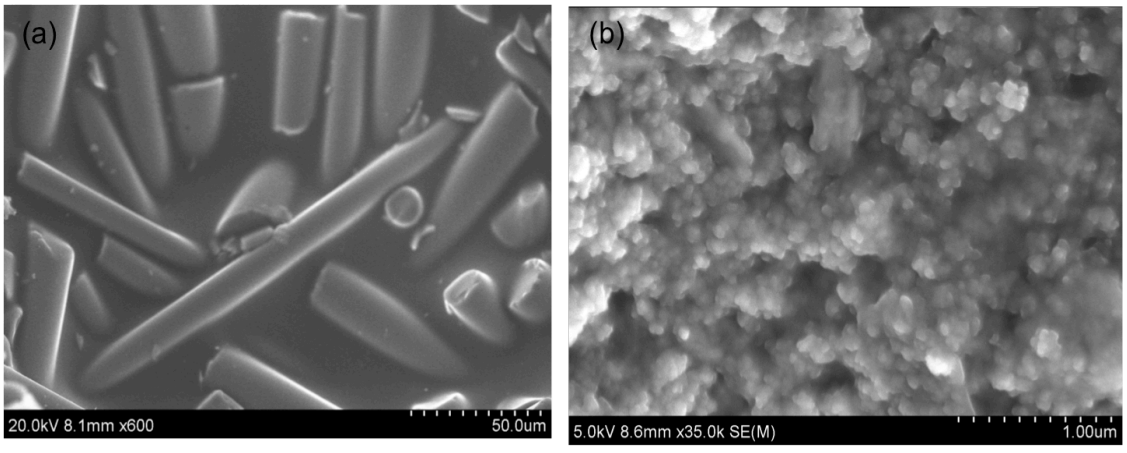

Figure 13: Composites organized using Injection Molding TO-4 (left) and Centrifuging TO-5 (right)

The surface of composites prepared by curing with and without controlled pressure is shown in Figure 13 (a) and (b) respectively. A significant decrease in surface porosity can be seen in figure 13 (b), the autoclave cured composite in comparison to 13 (a), which was cured under atmospheric pressure. It also increases the standard deviation in mechanical properties because pores don't support loads.

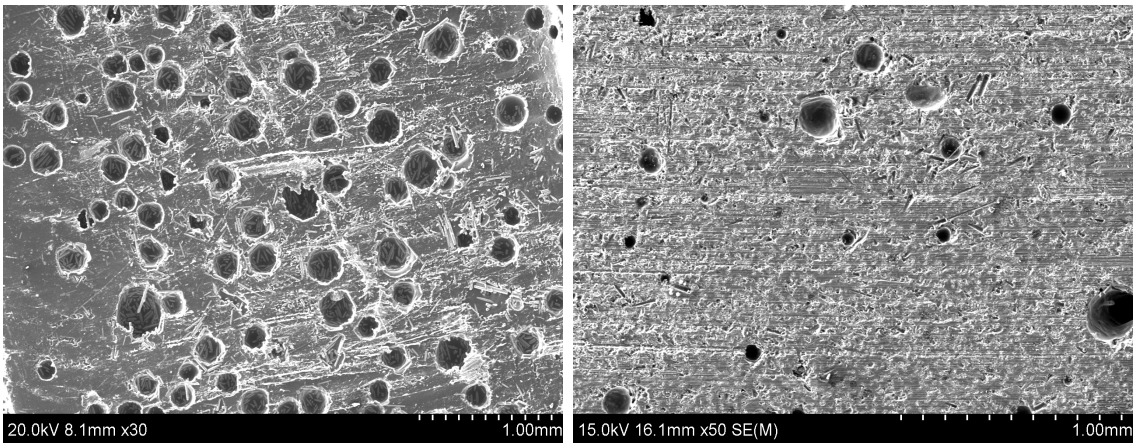

Figure 14: (a) curing without autoclave (b) curing with an autoclave

3.3 Mechanical characterization of reinforced composites

3.3.1 Vickers Hardness:

The Vickers hardness of composites with TO-4 and TO-5 fillers was measured after polishing. Table 5 shows the hardness and its standard deviation with respect to organization, curing approach, and filler type and loading level. Comparison with respect to the process of mixing, organizing and curing can be made using Table 5. Two trends are evident in Table 5. First, as would be expected, samples with higher filler loading have higher hardness than those with lower filler loading within the

same groups, unorganized or unorganized. Second, organized composites have a smaller standard deviation than unorganized composites with the smallest standard deviations for organized composites cured under pressure in the autoclave.

Table 5: Hardness and its standard deviation with respect to the organization and curing of the composite

	Filler	Vol. % filler	Organization	Curing	Vickers Hardness (HV)
1	TO-4	58	Unorganized	Room pressure	174 ± 45.6
2	TO-4	58	Unorganized	Autoclave	196± 81.2
3	TO-4	54	Organized (injection molding)	Autoclave	224 ± 7.33
4	TO-5	64	Unorganized	Room pressure	230 ± 71
5	TO-5	54	Organized (centrifuging)	Room pressure	194 ± 44
6	TO-5	53	Organized (injection molding)	Room pressure	185 ± 24.5
7	TO-5	53	Organized (injection molding)	Autoclave	176 ± 6.8

3.3.2 Three-point bend tests:

A limited number of tests were done to compare mechanical properties in organized and unorganized composites. Table 6 shows the results of these tests. TO-5 filler was used in both cases, but the unorganized composites had 58 vol% filler while the organized composites had 54 vol% filler. Table 6 shows that organizing the titanium oxide nanorods using the process of centrifugation had a significant effect on the fracture strength, fracture toughness and the Young's modulus of TO-5 reinforced composites. It can be seen from Table 6 that the unorganized composites had a lower Young's modulus with a larger standard deviation than the organized composites. The average flexural strength of the centrifuged composites is 80.5 MPa whereas the unorganized composites are 73.2 MPa. The composites all fractured in a brittle manner with the organized composites having a larger toughness than the unorganized composites.

Table 6: Strength, toughness and modulus values obtained from 3-point bend tests

	Sample	Modulus (MPa)	Flexural Strength (MPa)	Toughness (KJ/m^3)
Organized Composite (Centrifuged) Filler: TO-5 Volume %: 54	1	9050	90.1	1024
	2	8600	89.9	915
	3	8600	61.2	956
	Average	8750	80.5	965
	Standard Deviation	264	16.67	54
Unorganized Composite Filler: TO-5 Volume %: 58	1	6814	65.1	756
	2	8126	74.9	853
	3	8797	79.9	826
	Average	7913	73.2	812
	Standard Deviation	1008	7.5	50

The stress strain curves shown in Figure 14 show a significant difference between the unorganized and organized sample. Both the samples have undergone brittle fracture, but the area under the curve of the organized samples is higher than the organized sample.

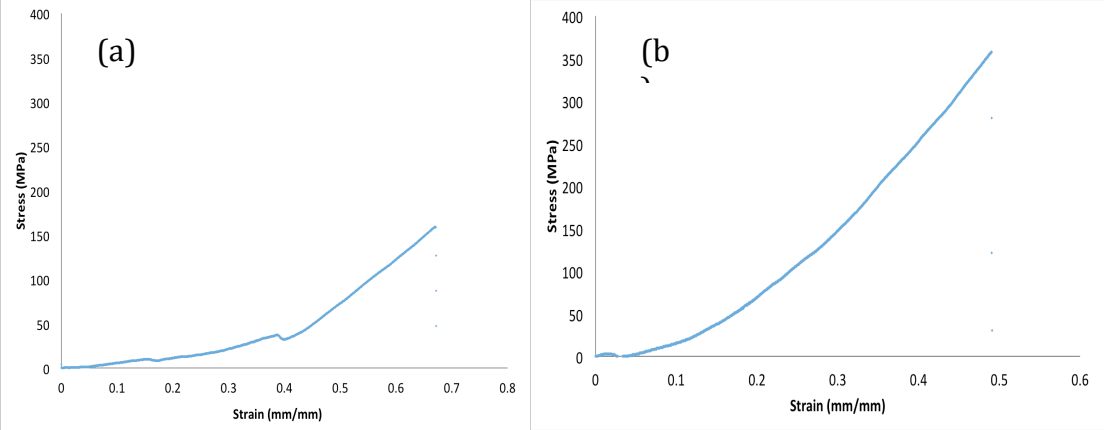

Figure 15: Stress- Strain Curves for (a) Unorganized Composite with 58 vol% To-5 and (b) organized Composite with 54 vol% TO-5 (loading direction was parallel to the alignment of rods)

Chapter 4

Discussion

4.1 Synthesis of 1D TiO_2:

4.1.1 Materials made from Ti metal powder

Compositions TO-1 to TO-4 were made using Ti metal powder and glycolic acid. The XRD data in Figure 7 and Table 3 indicate that glycolic acid concentration affects the crystallization of titanium dioxide in the autoclave. The XRD peaks for TO-1 in Figure 7 are much smaller and broader than those from TO-2 to TO-4 which had double the glycolic acid concentration. This indicates that TO-1 is not as well crystallized as TO-2 to TO-4, which is reflected in the smaller crystallite sizes, calculated for TO-1 in Table 3. Thus, the TO-2-TO-4 solutions autoclaved to grow the titania were less basic. The excess glycolic acid added after the sol-gel process and before the heat treatment in an autoclave appears to be responsible for the formation of 1D titania. It is hypothesized that the excess glycolic acid added inhibits growth of the crystal in certain directions and there is growth only in the active direction. This is due to selective adsorption of the excess glycolic acid as demonstrated by Kobayashi and Kato [38]. Adding ammonium tartrate or ammonium phosphate also affected the crystallization process. In composition TO-2, where no ammonium was added, both the metastable anatase phase and stable rutile phase are formed, while in compositions TO-3 and TO-4 only the rutile phase ~~is~~ formed in the presence of ammonium compounds. This indicates that the ammonium ions played a role in crystallization and growth processes of the powders. We hypothesize that the

ammonium ions helps to catalyze the titanium atoms to the formation of final bond network. This is supported by the work of Matteo et al. [39].

The SEM images of compositions TO-1 and TO-2 in Figure 9 demonstrate the effect of the excess glycolic acid addition after the gelling step in the sol-gel synthesis process. The diameter and length of the rods in Figure 9 was calculated using ImageJ software. Composition TO-2 which had average aspect ratio of as much as 70.5 was prepared using 3 wt% of excess glycolic acid while TO-1 had rods with an average aspect ratio of 1.5 was prepared using 1.5 wt% excess glycolic acid. This is due to selective adsorption of the excess glycolic acid. Facets chelated with glycolic acid will have a lower surface energy than the other faces as demonstrated by Kobayashi and Kato [38]. It appears that this preferred growth also limited agglomeration relative to TO-1. For both TO-1 and TO-2, we hypothesize that small nanocrystals aggregate to form nanorods during hydrothermal heating by the process of coarsening and oriented aggregation as proposed by Isley and Penn [40]. In compositions TO-3 and TO-4, ammonium tartrate and ammonium phosphate were also added respectively. Adding ammonium compounds is known to increase the rate of initial agglomeration of the nanocrystals during the formation of the rods [41]. Composition TO-4 had many rods that were bundled along the long axis. The presence of phosphate ions in TO-4 is believed to be responsible for this. Dan et al [42] proposed that the adsorption of phosphate ions on the particle surfaces could stabilize bundles. The ammonium ions present in TO-3 appear to promote the formation of hexagonal rods rather than round rods as in composition TO-4. TO-3 synthesized used ammonium tartarate had higher aspect ratio of 19.5 whereas TO-4 synthesized using

ammonium phosphate had an aspect ratio of 10.5. The lower aspect ratio of TO-4 was due to the adsorption of the phosphate ions on the surface [42].

4.1.2 Materials made from TTIP

Compositions TO-5 and TO-6 were prepared from TTIP and NaOH with TO-6 having twice as much NaOH in the solution as TO-5. Figure 8 and Table 2 show that TO-5 had much smaller crystallite size than TO-6 and that both compositions had anatase rather than rutile as the major phase. Figure 11 and Table 4 show that the extra NaOH added to TO-6 increased the anisotropy of the nanorods.. The standard deviation in the aspect ratio of TO-6 is around 10.2 with an aspect ratio of 17.9 where as standard deviation of TO-5 is 1.2 with an aspect ratio of 5.25. This is consistent with the behavior proposed by Martin et al [43] where the addition of NaOH inhibits crystallite growth upon heating for anatase phase during hydrothermal process [43]. The inhibition of growth was mainly in a single crystallographic direction, implying that the addition of NaOH can be utilized to enhance the control of size and morphology.

4.2 Mixing and organizing the composites:

Due to the high viscosity of the monomer, it was difficult to achieve a volume percentage of filler loading above 58 volume percent. Ethanol, which was used as diluent, not only helped in reducing the viscosity but it also helped in the organization of TiO_2 using injection molding and centrifuging.

Centrifugation was used to organize TO-5 filler in the monomer matrix with diluent. Centrifuging the composite after mixing by hand aided in uniformly

distributing the TiO_2 nanorods. In particular, it appeared to significantly reduce filler agglomeration. The organization of centrifuged rod-monomer mixture took place by gravity when the centrifuging tube was left in the hood for 72hrs for the evaporation of the diluent. While hardness was not affected, the standard deviation of the hardness values centrifuged and settled samples was significantly decreased as shown in Table 5. This was attributed to the more uniform distribution of rods in the centrifuged samples.

Injection molding aligned the microrods parallel to the extrusion direction as seen in Figure 12a. These rods start to get organized by the pressure applied at the nozzle during injection. The microrods get more organized during the passage through the pippette to the mold. The organization in the plane is not in a single direction because the rods entering the mold interact with each other. The standard deviation of the hardness in Table 5 is much smaller than that of similar unorganized composites. This indicates that rods in the injection molded composites, like those in the centrifuged and settled composites, were more uniformly distributed than in the unorganized composites.

4.3 Morphological characterization of the composites:

The uniform distribution of rods in the in the Bis-GMA and TEDGMA matrix for the injection molded 54 volume percent TO-4 (microrods) composites and the centrifuged 58 volume percent TO-5 (nanorods) was confirmed using SEM. As noted above and shown in Figure 12a, composites with TO-4 filler particles made by injection molding, demonstrated organization of filler in within a plane. In particular,

injection molding appeared to align most of the microrods in a plane parallel to the nozzle. The oriented composites had larger, more uniform hardness because of the distribution of the microrods. While it was not possible to observe nanorod organization in the SEM in composites filled with the TO-5 nanorods prepared by injection molding, is it likely that they would also have been homogenized and organized relative to the injection plane. The hardness values in Table 5 support this.

SEM observation of composites made with TO-5 using the process of centrifugation revealed that the nanorods are uniformly distributed in the matrix. From Figure 12b it can be seen that the nanorods are pointing towards the surface of the composite which is perpendicular to the axis of the centrifuging tube.

Porosity

The composites cured under atmospheric pressure had many large pores as shown in Figure 8a. As discussed below, these pores limited the mechanical properties. Although, the alcohol used as a diluent was allowed to evaporate for up to 72 hours, we believe that the residual porosity is related, as least in part, to alcohol that was not fully evaporated before curing. Some commercial composites are cured under pressure, and pressure would suppress the formation of large pores resulting from alcohol evaporation. Figure 11 show that curing in an autoclave decreased the total number of pores and the relative proportion of large pores. It was determined using SEM images that the porosity on the surface of the composite was decreased by autoclave curing.

4.4 Mechanical Characterization of the composites:

4.4.1 Vickers Hardness testing:

The hardness of polished composites was compared with respect to (i) mixing process of mixing (centrifuging to help break up agglomerates vs hand mixing), (ii) organization (injection molding vs. unorganized) and (iii) curing (atmospheric pressure vs. under controlled pressure in the autoclave). Table 5 shows the hardness and its standard deviation with respect to the organization and curing of the composites. TO-5 composites prepared by centrifuging and settling exhibited smaller standard deviations in the hardness than unorganized composite as seen in Table 5. The injection molded TiO-4 and TiO-5 composites also exhibited smaller standard deviations in hardness than unorganized composites. As noted above, this is believed to be a result of more uniform distribution of the nano- and micro-rods. In addition, composite 3 (injection molded, 54 vol% TO-4, autoclaved) had a much higher hardness than composites 1 and 2 (unorganized, 58 vl% TO-4, room pressure and autoclaved respectively). This indicates that injection molding is useful enhancing mechanical properties.

The non-uniformity in the hardness is due to the presence of pores. The presence of ethanol even after drying the composite is assumed to be the reason for the formation of pores during curing. This needs to be addressed before the composites developed in this research could be considered for applications as dental restorations. Autoclave curing decreases porosity per unit area in high volume percent filler composites. Composites with titania microrods (TO-4) fillers were used to compare an autoclave-cured composite with an to that of the air-cured prepared from

the same composition and batch. Table 5 shows that the hardness of the autoclaved samples was higher and more uniform. This can be attributed to the decrease in porosity.

4.4.2 Three Point Bend Tests:

The effect of organizing the TO-5 nanorod filler using centrifugation and settling on the flexural strength, Young's modulus and toughness was investigated by three point bending tests. First, unorganized composites prepared by mixing TO-5 into the monomer matrix with a spatula and then transferring them to molds was tested. The results are plotted in Figure 13. Then composites made by centrifuging and settling TO-5 filler (TO-5) in the monomer mixture were prepared, cured and tested. Table 6 and Figure 13 that the composites mixed with centrifugation have higher flexural strength, Young's modulus and toughness. The lower values for the unorganized composite indicate that centrifuging and settling has a significant effect on the distribution of nanorods in the matrix and the resulting mechanical properties. The data in Table 6 is the results of tests on three samples of each type. The shape of the strain curve shows that both samples types were brittle elastic solids.

Chapter 5

Conclusion and Future Work

5.1 Summary and conclusions:

TiO_2 micro- and nanorods were successfully synthesized using a template free and surfactant free sol-gel assisted hydrothermal processes. Varying the precursor material and processing parameters produced TiO_2 particles with different morphologies. Two of titanium oxide rod shaped powders developed were used to make composites with potential dental applications. Organizing the TiO_2 filler in the matrix using injection molding and centrifuging resulted in improvement of mechanical properties of the composite. Autoclave curing decreased the porosity. Our research findings are summarized as follows:

- Six different morphologies of TiO_2 were synthesized using two different routes:
  - (i) Powders TO-1 to TO-4: Titanium metal powder and glycolic acid were used as starting materials to form a titanium glycolate complex. Addition of excess glycolic acid resulted in the formation of TiO_2 rods of higher aspect ratios. Addition of ammonium phosphate during the process of synthesis resulted in uniformly sized and uniformly distributed bunches of TiO_2 micro-rods.
  - (ii) TTIP and oxalic acid were used as the starting material to form a titanium oxalate complex. NaOH was added to the precipitate the TiO_2. This process has resulted in the formation of uniform nanorods of 5-10nm in diameter and 40-45 nm in length. Addition of excess

NaOH during synthesis increased the anisotropy of the rods, but led to a non-uniform size distribution.

- Characterization of TiO_2 was conducted using XRD and SEM. According to the diffraction peaks of XRD, TiO_2 synthesized using titanium metallic powder as the starting material had rutile as the major phase whereas TiO_2 synthesized using TTIP as the starting material had anatase as the major phase.
- SEM images of the TiO_2 used to make the composites (TO-4 and TO-5) exhibited rod like structures with little agglomeration. Samples with uniform size distribution with no evidence of agglomeration were used to prepare the composites.
- TiO_2 was silanized and successfully incorporated into the 50:50 Bis-GMA and TEGDMA resin matrix.
- 1D TiO_2 was organized in the matrix using centrifugation and settling and injection molding. The hardness of the unorganized and the organized composites was measured using Vickers hardness and compared. Composites prepared by organizing the filler resulted in much more uniform hardness than the unorganized composite.
- Young's modulus, flexural strength and toughness were measured by 3-point bending for the unorganized and organized composites with centrifuged and settled TO-5 as the filler. The toughness, Young's modulus and flexural strength were found to be higher for the centrifuged and settled composite indicating that the organization of TiO_2 nanorods was beneficial.

- To decrease the porosity of the composites autoclave curing was investigated. SEM images of the composites cured under atmospheric pressure were compared with an autoclave-cured composite. A significant decrease in the amount of porosity was found.

5.2 Future Work

- The composites synthesized using bunches of TiO_2 microrods (TO-4) were not tested using 3-point bend test. If a larger amount of these rods can be synthesized, then testing bend bars made from TO-4 composites can show the effects of sizes and bundling on mechanical properties.
- Although use of injection molding has resulted in better hardness uniformity in the composites, the SEM images indicate there is no organization in the plane. If the flow of composite from the plastic tube can be controlled in the single direction, then the filler may also be organized in the plane. This would be helpful in mimicking enamel.
- As the polymerization shrinkage is expected to decrease in composites reinforced with TiO_2, these restorations could be tested in extracted teeth.
- These composites can be tested for biocompatibility in-vitro and in-vivo.

Works Cited

[1] Albers. "Tooth-colored restoratives: Principles and techniques." (2004): 10-61.

[2] McCabe JF, Walls A. Applied dental materials. 8th ed. Malden: MA: Blackwell Science, 1998.

[3] GJ, Knock FE. “Dental materials and methods”. Patent 2558139.

[4] RL, Bowen. "Properties of a silica-reinforced polymer for dental restorations. J Am Dent Assoc." J Am Dent Assoc. (1963): 57-64.

[5] A., Lindberg. "Resin composites: Sandwich restorations and curing techniques Umeå: Odontologi;." (2005).

[6] Hervas-Garcia A, Martinez-Lozano MA, Cabanes-Vila J, Barjau-Escribano A, Fos- Galve P. "Composite resins. A review of the materials and clinical indications." Med Oral Patol Oral Cir Bucal. (2006): 215-20.

[7] Dart EC, Cantwell JB, Traynor JR, Franciszek JJ, Nemeck J. Method of repairing teeth using a composition which is curable by irradiation with visible light. Patent 4089763. 1978.

[8] Seghi R. "Notes from Lecture 1 of DENT 430, Overview of Restorative Dentistry at Ohio State University,." Notes from Lecture 1 of DENT 430. 19 9 2011.

[9] Xue, J, et al. "X-ray microdiffraction, TEM characterization and texture analysis of human dentin and enamel." J Microscopy (2013): 144-153.

[10] Zheng, J, et al. "Microtribological behaviour of human tooth enamel and artificial hydroxyapatite." Tribology Intl (2013): 177-185.

[11] Hanning M, “Nanomaterials in preventive dentistry” Nature Nanotechnology volume 5, 565-569 (2010)

[12] Antonio Nanci, “Ten Cate's Oral Histology, 9th Edition”.

[13] Ferracane, J.L. "Current trends in dental composites." Critical Reviews in Oral Biology and Medicine, (1995): 302-318.

[14] Kundie, F, Che Husna A, Muchtar,A, “ Effects of filler size on the mechanical properties of polymer filled dental composites: A riview of recent developments”, Journal of Physical Science, Vol. 29(1), 141–165, 2018.

[15] Mitra SB, Wu D, Holmes BN. “An application of nanotechnology in advanced dentalmaterials”, The J of the Am Dent Ass. 2003;134(10):1382-90.

[16] Wagner HD, Vaia RA. “Nanocomposites: Issues at the interface”. Materials Today. 2004;7(11):38-42.

[17] “Lindberg A. Resin composites: Sandwich restorations and curing techniques”; Umeå: Odontologi; 2005

[18] Ilie N, Hickel R, Watts DC. “Spatial and cure-time distribution of dynamic-mechanical properties of a dimethacrylate nano-composite”, Dental Materials. 2009;25(3):411-18.

[19] Ilie N, Hickel R. “Macro-, micro- and nano-mechanical investigations on silorane and methacrylate-based composites”, Dental Materials. 2009;25(6):810-19.

[20] P. Kaur et al., “Tuning ferromagnetism in zinc oxide nanoparticles by chromium doping,” Appl. Nanosci., vol. 5, no. 8, pp. 975–981, 2015.

[21] Z. Zhang, Z. Kang, Q. Liao, X. Zhang, and Y. Zhang, “One-dimensional ZnO nanostructure-based optoelectronics,” Chinese Phys. B, vol. 26, no. 11, 2017.

[22] X. Luo, A. Morrin, A. J. Killard, and M. R. Smyth, “Application of nanoparticles in electrochemical sensors and biosensors,” Electroanalysis, vol. 18, no. 4, pp. 319–326, 2006.

[23] S. Sarkar, E. Guibal, F. Quignard, and A. K. SenGupta, “Polymer-supported metals and metal oxide nanoparticles: Synthesis, characterization, and applications,” J. Nanoparticle Res., vol. 14, no. 2, 2012.

[24] P. Cervantes-Avilés, E. Díaz Barriga-Castro, L. Palma-Tirado, and G. Cuevas-Rodríguez, “Interactions and effects of metal oxide nanoparticles on microorganisms involved in biological wastewater treatment,” Microsc. Res. Tech., vol. 80, no. 10, pp. 1103–1112, 2017.

[25] X. Wang, Z. Li, J. Shi, and Y. Yu, “One-dimensional titanium dioxide nanomaterials: Nanowires, nanorods, and nanobelts,” Chem. Rev., vol. 114, no. 19, pp. 9346–9384, 2014.

[26] S. León-Ríos et al., “One-Dimensional TiO 2 -B Crystals Synthesised by Hydrothermal Process and Their Antibacterial Behaviour on Escherichia coli,” J. Nanomater., vol. 2016, pp. 1–8, 2016.

[27] A. S. Nair, Z. Peining, V. J. Babu, Y. Shengyuan, and S. Ramakrishna, “Anisotropic TiO2 nanomaterials in dye-sensitized solar cells,” Phys. Chem. Chem. Phys., vol. 13, no. 48, p.

21248, 2011.

[28] S. Akbar, P. Dutta, and C. Lee, “High-temperature ceramic gas sensors: A review,” Int. J.Appl. Ceram. Technol., vol. 3, no. 4, pp. 302–311, 2006.

[29] K. Bubacz, B. Tryba, and A. W. Morawski, “The role of adsorption in

decomposition of dyes on TiO_2 and N-modified TiO_2 photocatalysts under UV and visible light irradiations," Mater. Res. Bull., vol. 47, no. 11, pp. 3697–3703, 2012.

[30] S. S. Lucky, N. Muhammad Idris, Z. Li, K. Huang, K. C. Soo, and Y. Zhang, "Titania coated upconversion nanoparticles for near-infrared light triggered photodynamic therapy," ACS Nano, vol. 9, no. 1, pp. 191–205, 2015.

[31] P. D. Cozzoli, M. L. Curri, C. Giannini, and A. Agostiano, "Synthesis of TiO2-Au composites by titania-nanorod-assisted generation of gold nanoparticles at aqueous/nonpolar interfaces," Small, vol. 2, no. 3, pp. 413–421, 2006.

[32] Y. Xia et al., "One-Dimensional Nanostructures: Synthesis, Characterization, and Applications," Adv. Mater., vol. 15, no. 5, pp. 353–389, Mar. 2003.

[33] H. J. Fan, P. Werner, and M. Zacharias, "Semiconductor nanowires: From self-organization to patterned growth," Small, vol. 2, no. 6, pp. 700–717, 2006.

[34] M. S. Program, "Oriented attachment and growth , twinning , polytypism , and formation of metastable phases : Insights from nanocrystalline TiO 2," vol. 83, pp. 1077–1082, 2000.

[35] J. Shi, C. Sun, M. B. Starr, and X. Wang, "Growth of titanium dioxide nanorods in 3D-confined spaces," Nano Lett., vol. 11, no. 2, pp. 624–631, 2011.

[36] Langford JI, Lou D. "Powder diffraction. Reports on Progress in Physics", Rep. Prog.Phys.1996;59(2):131

[34] Mohsen N, Craig R. "Effect of silanation of fillers on their dispersability by monomer systems", J Oral Rehabil. 1995;22(3):183-89.

[35] Yap AUJ, Mah MKS, Lye CPW, Loh PL. "Influence of Dietary Simulating Solvents on the Hardness of Provisional Restorative Materials", Dental Materials, 2004; 20: 370-376.

[36] Fultz B, Howe J. Transmission electron microscopy and diffractometry of materials. 4th ed. Springer Berlin Heidelberg, 2013; 115-117

[37] H. Jensen, J. H. Pedersen, J. E. Jorgensen, J. Skov Pedersen, K.D Joensen, S.B. Iversen, E.G. Sogaard, 2006. J. of Experiemental Nanoscience, 1:355.

[38] M. S. Program, "Oriented attachment and growth , twinning , polytypism , and formation of metastable phases : Insights from nanocrystalline TiO_2," vol. 83, pp. 1077–1082, 2000.

[39] Matteo C, Thomas, and Christopher B. M. "Solution-Phase Synthesis of Titanium Dioxide Nanoparticles and Nanocrystals", Chem. Rev. 2014, 114, 9319−9345

[40] J. Shi, C. Sun, M. B. Starr, and X. Wang, "Growth of titanium dioxide nanorods in 3D-confined spaces," Nano Lett., vol. 11, no. 2, pp. 624–631, 2011.

[41] M. Kobayashi,H. Kato and M. Kakihana, "Synthesis of Titanium Dioxide Nanocrystals with Controlled Crystal- and Micro-structures from Titanium Complexes", Nanometor. nanotechnol., 2013 Vol.3, Article. 23

[42] Sara L, Isley, and R. Lee Penn, "Titanium Dioxide Nanoparticles: Effect of Sol-Gel pH on Phase Composition, Particle Size, and Particle Growth Mechanis" . Phys.

Chem. C, 2008, 112 (12), pp 4469–4474.

[43] Martin S, Yanbin S, and Bo B, “Iversen TiO2 Nanoparticles for Li-Ion Battery Anodes: Mitigation of Growth and irreversible capacity using LiOH and NaOH”, chem matter, 2015, 27, 119-126.

[44] Mohsen N, Craig R, “Effect of silanation of fillers on their dispersability by monomer systems”, J Oral Rehabil. 1995;22(3):183-89.

[45] Wilson KS, Zhang K, Antonucci JM. "Systematic variation of interfacial phase reactivity in dental nanocomposites." Biomaterials (2005): 26(25):5095-103.